

## Enhanced red phosphorescence in nanosized $\text{CaTiO}_3\text{:Pr}^{3+}$ phosphors

Xianmin Zhang, Jiahua Zhang, Zhaogang Nie, Meiyuan Wang, Xinguang Ren et al.

Citation: *Appl. Phys. Lett.* **90**, 151911 (2007); doi: 10.1063/1.2722205

View online: <http://dx.doi.org/10.1063/1.2722205>

View Table of Contents: <http://apl.aip.org/resource/1/APPLAB/v90/i15>

Published by the American Institute of Physics.

---

### Related Articles

Impact of resonator geometry and its coupling with ground plane on ultrathin metamaterial perfect absorbers  
*Appl. Phys. Lett.* **101**, 101102 (2012)

Control of reflectance and transmittance in scattering and curvilinear hyperbolic metamaterials  
*Appl. Phys. Lett.* **101**, 091105 (2012)

Discontinuous design of negative index metamaterials based on mode hybridization  
*Appl. Phys. Lett.* **101**, 081913 (2012)

Metamaterial filter for the near-visible spectrum  
*Appl. Phys. Lett.* **101**, 083106 (2012)

A fast Fourier transform implementation of the Kramers-Kronig relations: Application to anomalous and left handed propagation  
*AIP Advances* **2**, 032144 (2012)

---

### Additional information on *Appl. Phys. Lett.*

Journal Homepage: <http://apl.aip.org/>

Journal Information: [http://apl.aip.org/about/about\\_the\\_journal](http://apl.aip.org/about/about_the_journal)

Top downloads: [http://apl.aip.org/features/most\\_downloaded](http://apl.aip.org/features/most_downloaded)

Information for Authors: <http://apl.aip.org/authors>

## ADVERTISEMENT



**HAVE YOU HEARD?**

Employers hiring scientists  
and engineers trust  
**physicstodayJOBS**

<http://careers.physicstoday.org/post.cfm>



## Enhanced red phosphorescence in nanosized $\text{CaTiO}_3\text{:Pr}^{3+}$ phosphors

Xianmin Zhang, Jiahua Zhang,<sup>a)</sup> Zhaogang Nie, Meiyuan Wang, and Xinguang Ren  
Key Laboratory of Excited State Processes, Changchun Institute of Optics, Fine Mechanics and Physics (CIOMP), Chinese Academy of Sciences(CAS), 16 Eastern South Lake Road, Changchun 130033, China and Graduate School of Chinese Academy of Sciences, Beijing 100039, China

Xiao-jun Wang<sup>b)</sup>  
Key Laboratory of Excited State Processes, CIOMP, CAS, Changchun 130033, China  
and Department of Physics, Georgia Southern University, Statesboro, Georgia 30460

(Received 9 January 2007; accepted 10 March 2007; published online 11 April 2007)

The red photoluminescence and phosphorescence originating from  $^1D_2\text{-}^3H_4$  transition of  $\text{Pr}^{3+}$  in  $\text{CaTiO}_3$  nanoparticles are studied as a function of  $\text{Pr}^{3+}$  concentrations. The nanophosphors exhibit both longer persistence time of 30 min and higher quenching concentration of 0.4 mol % than the bulk (10 min and 0.1 mol %). The initial phosphorescence in the nanophosphor is an order of magnitude stronger than that in the bulk at the corresponding quenching concentrations. Phosphorescence decay patterns and diffused reflectance spectra before and after ultraviolet exposure indicate the existence of more traps contributing to phosphorescence in the nanoparticles. © 2007 American Institute of Physics. [DOI: 10.1063/1.2722205]

Long persistent phosphorescent materials have attracted considerable attention for various displays and signing applications in dark environments.<sup>1–5</sup> Some oxide persistent phosphors exhibiting high brightness of blue and green phosphorescence with better chemical stability over sulfides are commercially available.<sup>1,2</sup> However, commercial red emitting oxide persistent phosphors with long persistence time have not been obtained yet. Red emitting phosphors of  $\text{CaTiO}_3\text{:Pr}^{3+}$  with excellent chemical stability and ideal color purity have been extensively investigated.<sup>6–9</sup> In 1997, red phosphorescence in  $\text{CaTiO}_3\text{:Pr}^{3+}$  codoped with MgO or ZnO was observed.<sup>10</sup> Recently, Haranath *et al.*<sup>11</sup> reported the phosphorescence enhancement of  $(\text{Ca,Zn})\text{TiO}_3\text{:Pr}^{3+}$  by adding nanosized silica powders to passivate the surface of the host to minimize the concentration of the undesirable defects. In our previous work,<sup>12,13</sup> the enhancement of fluorescence and phosphorescence intensities of  $\text{CaTiO}_3\text{:Pr}^{3+}$  was realized by adding rare earth ions  $\text{Ln}^{3+}$  ( $\text{Ln}=\text{La,Lu,Gd}$ ) in the phosphors to perform charge self-compensation to suppress  $\text{Ca}^{2+}$  and  $\text{Ti}^{4+}$  vacancies, and consequently, to significantly increase the fluorescence emission efficiency.

On the other hand, the density of traps plays an essential role in the persistence of phosphorescence materials.<sup>3</sup> Conventionally, traps can be created by charge defects or by incorporating with auxiliary activators into host.<sup>1,2,14–17</sup> To improve the phosphorescence intensity and persistent time, the increase of the density of traps in the host is needed. In nanosized phosphors, there exist numerous surface due to the defects on their surfaces due to the large surface to volume ratio, which generally act as luminescent killers,<sup>18,19</sup> some of which, however, can probably act as traps beneficial for the generation of phosphorescence.

In this letter, we report the enhancement of phosphorescence in nanosized  $\text{CaTiO}_3\text{:Pr}^{3+}$  phosphors prepared by sol-gel methods. It is observed that the phosphorescence intensities in the nanoparticles can be one order of magnitude

higher than that in the bulk powders in the initial decay period, which is attributed to the existence of a large amount of surface traps in the nanoparticles.

0.01M  $\text{CaCl}_2$ , 0.01M citric acid ethanol solution, and  $\text{PrCl}_3$  solution ( $\text{Pr}_6\text{O}_{11}$  was dissolved in HCl) were mixed. The molar ratio of  $\text{Ca}^{2+}$  to  $\text{Pr}^{3+}$  was in the range from 1:0.02% to 1:1%. Under constant magnetic stirring,  $\text{Ti}(\text{OC}_4\text{H}_9)_4$  was slowly added until yellow sol was obtained. By heating at 100 °C for 10 h, the sol changed to gel. After further firing at 300 °C for 2 h, a dark solid mass was obtained. When it was cooled to room temperature, it was ground into powder. White nanosized  $\text{CaTiO}_3\text{:Pr}^{3+}$  particles were obtained after sintering the black powder at 600 °C for 2 h in air. The bulk powder was synthesized by conventional solid state reaction at 1400 °C for 3 h in air.<sup>12,13</sup>

The structural characterization was analyzed by x-ray diffraction (XRD; Rigaku D/max-rA) spectra with the Cu  $K\alpha$  line of 1.540 78 Å. The morphology of products was observed by field emission scanning electron microscopy (Hitachi S-4800). Photoluminescence (PL), PL excitation (PLE), diffused reflectance spectra ( $\text{BaSO}_4$  sample was used as a standard), and phosphorescence decay curves were measured using a Hitachi F-4500 fluorescence spectrophotometer. Fluorescence and phosphorescence were measured after irradiation by 365 nm ultraviolet (UV) light for 10 min.

Figure 1 shows the XRD patterns of  $\text{CaTiO}_3\text{:0.4 mol \% Pr}^{3+}$  nanoparticles and  $\text{CaTiO}_3\text{:0.1 mol \% Pr}^{3+}$  bulk powder. The identical XRD patterns of the two samples suggest the same crystal structure of the nanoparticles as the bulk one, being orthorhombic (JCPDS Card No. 82–0228). Due to size effect, the nanoparticles exhibit larger widths of the XRD peaks than the bulk.<sup>19</sup> By applying Scherrer's formula with the measured widths of the XRD peaks, the average size of 27.5 nm for  $\text{CaTiO}_3\text{:0.4 mol \% Pr}^{3+}$  nanoparticles is estimated, which is close to the uniform size value of 30 nm determined from the scanning electron microscope (SEM) image as shown in the inset of Fig. 1. The particle size of the bulk powder is around 2  $\mu\text{m}$ .

PL and PLE spectra of  $\text{CaTiO}_3\text{:Pr}^{3+}$  nanoparticles with different concentrations of  $\text{Pr}^{3+}$  are presented in Fig. 2,

<sup>a)</sup>Electronic mail: zhangjh@ciomp.ac.cn

<sup>b)</sup>Electronic mail: xwang@georgiasouthern.edu

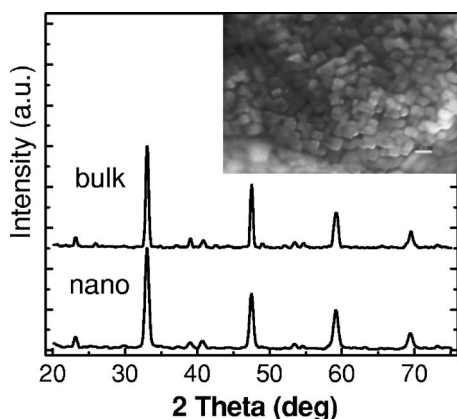


FIG. 1. Powder XRD patterns of  $\text{CaTiO}_3:\text{Pr}^{3+}$  for nanoparticles ( $\text{Pr}^{3+}$ :0.4 mol %) and bulk sample ( $\text{Pr}^{3+}$ :0.1 mol %). Inset: The SEM image of nanoparticles.

where the curve for bulk powders ( $\text{Pr}^{3+}$ :0.1 mol %) is also plotted for comparison. The PL spectra show a red emission line at 615 nm, originating from intra- $4f^1D_2 \rightarrow 3H_4$  transition of  $\text{Pr}^{3+}$ .<sup>6</sup> The PLE spectra monitoring the red emission mainly consist of two broad bands (A and B) in the UV region, which are located at 319 nm (A) and 265 nm (B), respectively. In comparison with the spectra of  $\text{CaTiO}_3:\text{Pr}^{3+}$  bulk powder (dashed line), band A shifts from 330 nm in the bulk to 319 nm in the nanoparticles. The position of band A is experimentally observed to be consistent with that of the band edge absorption of  $\text{CaTiO}_3$  host due to  $\text{O}(2p)\text{-Ti}(3d)$  transition<sup>6</sup> (see Fig. 5), indicating that the blueshift of band A in the nanoparticles is the result of size confinement effect, which was also observed in  $\text{CaTiO}_3:\text{Pr}^{3+}$  thin films.<sup>20</sup> The band B exhibiting no obvious shift in the nanoparticles is attributed to the  $4f^2 \rightarrow 4f5d$  absorption of  $\text{Pr}^{3+}$  ions.<sup>9</sup>

Figure 3 depicts the dependence of luminescence intensities (a) and initial phosphorescence intensities (b) on  $\text{Pr}^{3+}$  concentrations in  $\text{CaTiO}_3:\text{Pr}^{3+}$  nanoparticles (shaded bars) and in the bulk powder (empty bars). One can find that there appears the same quenching concentration for luminescence and phosphorescence, but the quenching concentration for the nanoparticles is different from that for the bulk powder.

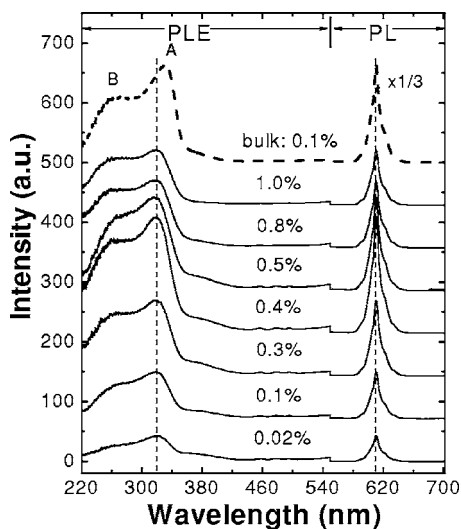


FIG. 2. PL and PLE spectra of  $\text{CaTiO}_3:\text{Pr}^{3+}$  for nanoparticles with different  $\text{Pr}^{3+}$  concentrations (0.02–1.0 mol %) and a bulk sample with 0.1 mol %  $\text{Pr}^{3+}$ .

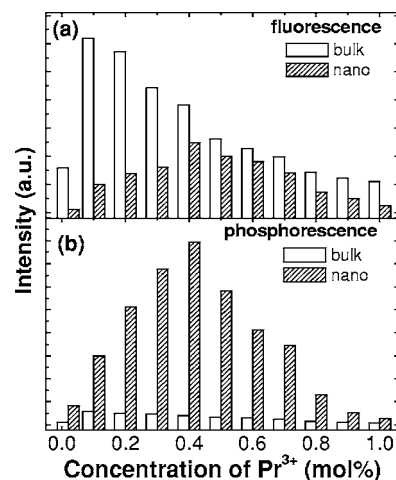


FIG. 3. Fluorescence (a) and phosphorescence (b) intensities of  $\text{CaTiO}_3:\text{Pr}^{3+}$  at various  $\text{Pr}^{3+}$  concentrations for nanoparticles (shaded bars) and bulk samples (empty bars), respectively. Fluorescence is detected by exciting into the strong absorption band of the host at 319 nm for the nanoparticles and at 330 nm for the bulk.

The quenching concentration of  $\text{Pr}^{3+}$  is around 0.4 mol % in the nanoparticles, quite higher than that of 0.1 mol % in the bulk. To explain this result, the deficiency of traps due to the limited primitive cells per particle as well as the hindrance of energy transfer of the particle boundary are considered to be responsible for the size dependence of quenching concentrations, as has been discussed in the literature.<sup>19</sup> The more significant phenomenon presented in Fig. 3 is the remarkable enhancement of phosphorescence in nanosized  $\text{CaTiO}_3:\text{Pr}^{3+}$ . It is found that although the luminescence intensities in the nanoparticles are lower than that in the bulk, the phosphorescence in the nanoparticles appears more intense than that in the bulk materials. It is exhibited that the maximum of the phosphorescence intensities in the nanoparticles is one order of magnitude higher than that in the bulk samples.

Figure 4 illustrates the time decay curves of phosphorescence in  $\text{CaTiO}_3$ :0.4 mol %  $\text{Pr}^{3+}$  nanoparticles (curve a) and  $\text{CaTiO}_3$ :0.1 mol %  $\text{Pr}^{3+}$  bulk powder (curve b) after irradiation with 365 nm UV light for 10 min. A larger integrated area under the decay curve of the nanosized sample than that of the bulk is demonstrated, indicating large photon storage capacity in nanosized phosphors, which exhibits >30 min persistence time detected by eyes, longer than that of the bulk sample ( $\sim 10$  min). The photon storage capacity of persistent phosphors is related to the density of traps. Due to the large surface to volume ratio, nanoparticles possess more

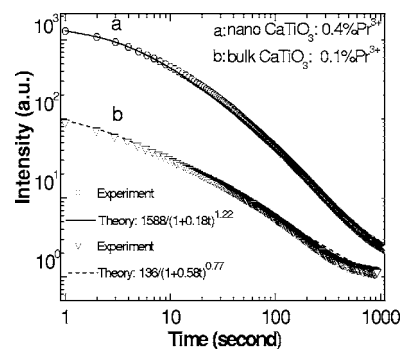


FIG. 4. Phosphorescence decay curves of  $\text{CaTiO}_3:\text{Pr}^{3+}$  for nanoparticles and bulk powders after irradiation by 365 nm UV light for 10 min.

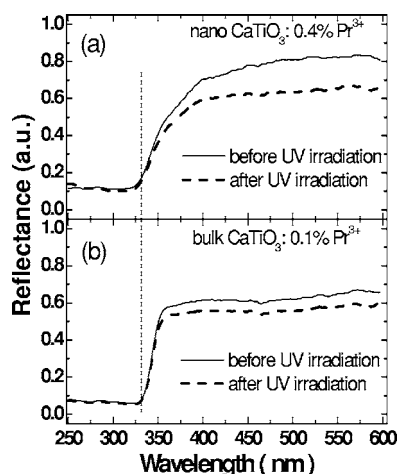


FIG. 5. Diffused reflectance spectra of  $\text{CaTiO}_3:\text{Pr}^{3+}$  for nanoparticles (a) and bulk sample (b) before (solid lines) and after (dashed lines) 365 nm UV-light irradiation for 10 min.

density of defects on their surfaces than the bulk. These defects may contribute to quenching of  $\text{Pr}^{3+}$  luminescence and/or trapping of electron or holes generated by UV excitation. This consequently suppresses the luminescence, but enhances the phosphorescence of nanosized  $\text{CaTiO}_3:\text{Pr}^{3+}$  phosphors. One can find that the decay curves can be fitted well by the following hyperbolic curve, indicating that the phosphorescence process meets a second-order mechanism:<sup>21</sup>

$$I(t) = I_0 / (1 + \gamma t)^n, \quad (1)$$

where  $I(t)$  and  $I_0$  are the phosphorescence intensities at time  $t$  and 0, respectively,  $\gamma$  is the mean decay rate, and  $n$  is a constant around 0.5–2. The fitting yields the mean decay rates  $\gamma$  to be  $0.18 \text{ s}^{-1}$  for the nanoparticles and  $0.58 \text{ s}^{-1}$  for the bulk;  $\gamma$  is inversely proportional to the amount of the trapping centers in the host.<sup>21</sup> A smaller mean decay rate in the nanoparticles, therefore, is a reflection of more trapping centers in the nanoparticles than that in the bulk, as we expected. This expectation is also confirmed with the diffused reflectance spectra of  $\text{CaTiO}_3:\text{Pr}^{3+}$  nanoparticles and bulk powder before and after 365 nm UV-light irradiation for 10 min, as shown in Fig. 5. Strong absorption edges of the host at around 319 nm [Fig. 5(a)] for nanoparticles and at 330 nm [Fig. 5(b)] for bulk powder are clearly presented, in good agreement with the position of the corresponding band A observed in the PLE spectra of Fig. 2. In Fig. 5 both nanosized and bulk materials exhibit extra absorbance in the range of 350–600 nm after irradiation with 365 nm for 10 min. It is experimentally observed that the enhanced absorbance recovers in synchronism with the decay of phosphorescence, suggesting that the UV irradiation induced op-

tical absorption is originated from the filled traps. We can see in Fig. 5 that the increment of absorbance in the visible range in the nanoparticles is much larger than that in the bulk powder, further indicating more traps in the nanoparticles. It should be noted that the difference of diffuse reflectance between 0.8 of the nanoparticles and 0.6 of the bulk around 600 nm before irradiation is due to the existence of more Ca and Ti vacancies in the bulk,<sup>13</sup> formed during the preparation at high sintering temperature of  $1400^\circ\text{C}$ .

In conclusion, nanosized  $\text{CaTiO}_3:\text{Pr}^{3+}$  phosphors demonstrate stronger and longer phosphorescence than the bulk samples due to the existence of high density traps on their surface resulting from the high surface to volume ratio in nanomaterials. This work provides a promising approach for improving long lasting persistent phosphors using nanotechnology.

This work is financially supported by the MOST of China (Nos. 2006CB601104 and 2006AA03A138) and the National Natural Science Foundation of China (Nos. 10574128 and 10504031).

- <sup>1</sup>T. Matsuzawa, Y. Aoki, N. Takeuchi, and Y. Murayama, *J. Electrochem. Soc.* **143**, 2670 (1996).
- <sup>2</sup>W. Jia, H. Yuan, L. Lu, H. Liu, and W. M. Yen, *J. Cryst. Growth* **200**, 179 (1999).
- <sup>3</sup>D. Jia, R. S. Meltzer, W. M. Yen, W. Jia, and X. J. Wang, *Appl. Phys. Lett.* **80**, 1535 (2002).
- <sup>4</sup>X. J. Wang, D. Jia, and W. M. Yen, *J. Lumin.* **102-103**, 34 (2003).
- <sup>5</sup>C. Y. Li and Q. Su, *Appl. Phys. Lett.* **85**, 2190 (2004).
- <sup>6</sup>P. T. Diallo, P. Boutinaud, R. Mahiou, and J. C. Cousseins, *Phys. Status Solidi A* **160**, 255 (1997).
- <sup>7</sup>H. Yamamoto, S. Okamoto, and H. Kobayashi, *J. Lumin.* **100**, 325 (2002).
- <sup>8</sup>Y. X. Pan, Q. Su, H. F. Xu, T. H. Chen, W. K. Ge, C. L. Yang, and M. M. Wu, *J. Solid State Chem.* **174**, 69 (2003).
- <sup>9</sup>X. M. Liu, P. Y. Jia, J. Lin, and G. Z. Li, *J. Appl. Phys.* **99**, 124902 (2006).
- <sup>10</sup>M. R. Royce and S. Matsuda, U.S. Patent No. 5,656,094 (July 22, 1997).
- <sup>11</sup>D. Haranath, A. F. Khan, and Harish Chander, *Appl. Phys. Lett.* **89**, 091903 (2006).
- <sup>12</sup>X. M. Zhang, J. H. Zhang, X. Zhang, C. Li, S. Z. Lu, and X. J. Wang, *J. Lumin.* **122-123**, 958 (2007).
- <sup>13</sup>X. M. Zhang, J. H. Zhang, C. Li, Y. S. Luo, and X. J. Wang, *Chem. Phys. Lett.* **434**, 237 (2007).
- <sup>14</sup>D. Jia, X. J. Wang, and W. M. Yen, *Chem. Phys. Lett.* **363**, 241 (2002).
- <sup>15</sup>Y. H. Lin, Z. L. Tang, Z. T. Zhang, and C. W. Nan, *Appl. Phys. Lett.* **81**, 996 (2002).
- <sup>16</sup>B. Liu, C. S. Shi, and Z. M. Qin, *Appl. Phys. Lett.* **86**, 191111 (2005).
- <sup>17</sup>Y. L. Liu, B. F. Lei, and C. S. Shi, *Chem. Mater.* **17**, 2108 (2005).
- <sup>18</sup>B. M. Tissue, *Chem. Mater.* **10**, 2837 (1998).
- <sup>19</sup>Z. G. Wei, L. D. Sun, C. S. Liao, J. L. Yin, X. C. Jiang, and Y. C. Hua, *J. Phys. Chem. B* **106**, 10610 (2002).
- <sup>20</sup>P. Boutinaud, E. Tomasella, A. Ennajaoui, and R. Mahiou, *Thin Solid Films* **515**, 2316 (2006).
- <sup>21</sup>S. Shionoya and W. M. Yen, *Phosphors Handbook* (CRC, Boca Raton, FL, 1999), Chap. 2, p. 91.